CrossMark
click for updates

Investigation of reactive species using various gas plasmas†

Toshihiro Takamatsu,[*ab] Kodai Uehara,[a] Yota Sasaki,[a] Hidekazu Miyahara,[a] Yuriko Matsumura,[c] Atsuo Iwasawa,[c] Norihiko Ito,[d] Takeshi Azuma,[b] Masahiro Kohno[c] and Akitoshi Okino[a]

In this study, atmospheric nonequilibrium plasmas were generated with six gas species using a multi-gas plasma jet. Singlet oxygen, OH radicals, H radicals, and NO radicals, in reaction with a solution interface, were measured using electron spin resonance. Carbon dioxide plasma generated the largest amount (90 μM) of singlet oxygen at 30 s, and argon-containing vapor gas plasma generated the largest amount (210 μM) of OH radicals. Among the homo-atomic gas species, nitrogen plasma generated the largest amount (130 μM) of OH radicals. In addition, H radicals were generated with argon, helium, and nitrogen plasmas. NO radicals were generated with nitrogen–oxygen plasma, and the largest amount of NO radicals was generated at a 1 : 1 volume ratio. These measurement results of the reactive species generated by individual gas plasmas permit identification of the production processes of reactive species.

Introduction

Atmospheric-pressure plasma shows strong industrial potential because it enables continuous treatment with a high-density of reactive species without the need for exhaust or pumping devices. Plasma processes have been studied in various fields including semiconductor processing,[1] harmful gas decomposition,[2] toxic degradation,[3] and elemental analysis.[4–7] In recent years, even heat-sensitive materials such as the human body have been treated with plasma, since argon and helium plasma can be generated at room temperature to 100 °C by nonequilibrium plasma. The use of nonequilibrium plasma has been confirmed to effectively inactivate *Escherichia coli* (*E. coli*) and *Bacillus subtilis*,[8] cause blood coagulation,[9,10] and kill cancer cells;[11,12] therefore, these promising applications have attracted attention in medical fields. In particular, clinical tests are underway for wound healing and prevention of wound infection,[13,14] since the microorganism inactivation effect by plasma can kill all associated microorganisms. Since these effects are observed in the presence of water, discussions only in the case of reactive species generated in the gas phase are insufficient. The reaction of reactive species at the liquid surface is an important consideration. In particular, reactive species such as singlet oxygen, OH radicals, and NO radicals generated by plasma in liquid are considered to have a vital relationship to the mechanisms involved.[15] For example, Oehmigen *et al.* have suggested that the inactivation effect of plasma on *E. coli* in liquid is caused by the production of reactive oxygen species (ROS) and reactive nitrogen species (RNS) such as OH radicals, NO radicals, nitrites, and peroxynitrous acids (ONOOH).[16] However, common method such as photometric measurement is difficult to identify the reactive species, thus there is few report to detect the individual ROS and RNS in the aqueous solution. The knowledge both of the quantity and the kind of ROSs and RNSs generated by the plasma treatment is useful to dissolve the problem of the microorganism inactivation mechanism. Therefore, electron spin resonance (ESR) has been used to measure the reactive species generated in liquid.[17] However, conventional plasma sources are limited in their abilities to generate gas species. They can only generate air and argon plasmas, where argon plasma is relatively easy to generate. The reaction processes and production amounts of reactive species are not yet well verified. Our group succeeded in developing a multi-gas plasma jet,[18–20] which can generate plasma from various gas species. Using this plasma source, reactive species can be investigated in detail, since they can be generated selectively by the supplied gas species. This study aims to clarify the relationships between the amount of reactive species and the gas species, and to consider the reaction process at the gas–liquid interface.

aDepartment of Energy Sciences, Tokyo Institute of Technology, Yokohama, Japan. E-mail: toshihiro@plasma.es.titech.ac.jp

bDepartment of Gastroenterology, Kobe University, Kobe, Japan

cDepartment of Bioengineering, Tokyo Institute of Technology, Yokohama, Japan

dVeterinary Medical Center, Tottori University, Tottori, Japan

Experimental setup

The multi-gas plasma jet can generate stable atmospheric plasma of various types of gas species such as argon, oxygen,

nitrogen, carbon dioxide, mock air, and their mixtures at low gas temperatures.[18–20] The body of the device is grounded and an interior high-voltage electrode is connected to an AC power supply (Plasma Concept Tokyo, Inc.) of 16 kHz and 9 kV. The generated plasma flows through a 1 mm hole with a flow rate of 1 L min^{-1}. It has been found that the plasma gas temperature was indicated as below 50 °C at 5 mm from the outlet using thermocouple measurement, and the plasma power was calculated as 10 W from voltage and current measurement.[18,19]

Each reactive species reacts with individual spin-trapping agents, and the spin adducts can be identified using ESR. In this study, the spin-trapping agents include 2,2,5,5-tetramethyl-3-pyrroline-3-carboxamide (TPC) as the singlet oxygen detector,[21] 5,5-dimethyl-1-pyrroline-N-oxide (DMPO) as the OH radical and H radical detector,[22] and N-methyl-D-glucamine dithiocarbamate iron (MGD-Fe) as the NO radical detector.[23] These agents were dissolved in a phosphate-buffered saline (PBS)(−) solution, with a pH value of 7.3–7.5, and the concentrations of TPC, DMPO, and MGD-Fe were fixed at 75, 200, and 8 mM, respectively (consult the ESI†). ESR was set at a 9.424818 GHz microwave frequency, a 2 min sweep time, and 100 kHz modulation frequency. The conditions for measuring TPC and DMPO included a magnetic field of 335.5 ± 5 mT, a modulation width of 0.1 mT, and a time constant of 0.1 s. The conditions for measuring MGD-Fe included a magnetic field of 330 ± 5 mT, a modulation width of 0.7 mT, and a time constant of 0.3 s.

We investigated each reactive species generated by the plasmas of argon, helium, mock air ($N_2 : O_2 = 8 : 2$), nitrogen, oxygen, and carbon dioxide using TPC, DMPO, and MGD-Fe. Plasma treatments of 200 μL solutions were operated at a distance of 6 mm from the plasma source outlet to the liquid surface for 30 s, as illustrated in Fig. 1. The amounts of reactive species generated was calibrated with spin adducts of 2,2,6,6-tetramethylpiperidine 1-oxyl, for which the radical amount was known. TPC can be oxidized by reactive species other than singlet oxygen; therefore, we used sodium azide (NaN$_3$),[21] which is known to be a scavenger of singlet oxygen. The concentration of NaN$_3$ was fixed at 100 mM, and the spin adducts of the combined treated TPC and NaN$_3$ solution were compared with the spin adducts of a solution containing treated TPC only.

For measuring singlet oxygen, we investigated H and OH radicals, as well as their production amounts by vapour (H$_2$O)-added argon gas plasma. In addition, with respect to the oxygen–nitrogen plasma, we measured the amounts of singlet oxygen, OH radicals, and NO radicals generated at various gas mixture rates.

Result

Measurement of singlet oxygen

TPC (75 mM) and TPC (75 mM) + NaN$_3$ (100 mM) solutions were treated with each gas plasma, and the amounts of singlet oxygen generated were calculated from the differences in the ESR signals. Results show that the carbon dioxide plasma generated the largest amount of singlet oxygen, as shown in Fig. 2. The amount of singlet oxygen generated by the carbon dioxide plasma was estimated to be 90 μM, from the difference between the ESR measurements of 210 μM for the TPC solution and 120 μM for the TPC + NaN$_3$ solution. The amount of singlet oxygen generated by oxygen plasma was estimated to be 63 μM, from the difference between the ESR measurements of 94 μM for the TPC solution and 31 μM for the TPC + NaN$_3$ solution. The rate of the singlet oxygen reduction by NaN$_3$ compared with the rate using TPC only, which is generated by oxygen plasma, was larger than the singlet oxygen reduction rate generated by other gas plasmas. The amount of spin, measured with the TPC + NaN$_3$ solution, was insignificant, although spin adducts of singlet oxygen were observed in the TPC solutions treated by other gas species. Therefore, we suspect that the spin adducts are caused by other ROS.

Measurement of OH and H radicals

DMPO (200 mM) solutions were treated with each gas plasma, and the amounts of OH and H radicals were calculated from the ESR signal. Our results show that Ar + H$_2$O plasma generated the largest amount of OH radicals, at 210 μM, as shown in Fig. 3. Among the monatomic gas species, nitrogen plasma generated the largest amount of OH radicals, at 130 μM. OH radical production by argon, helium, oxygen, and carbon dioxide plasmas were 84, 68, 32, and 28 μM, respectively. The H radical
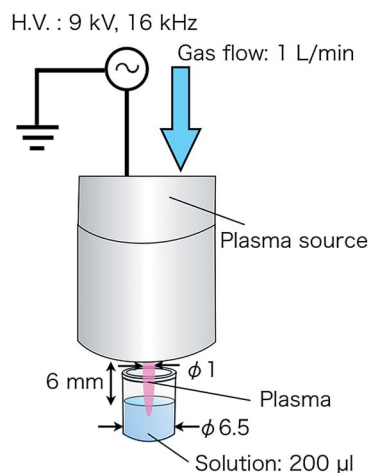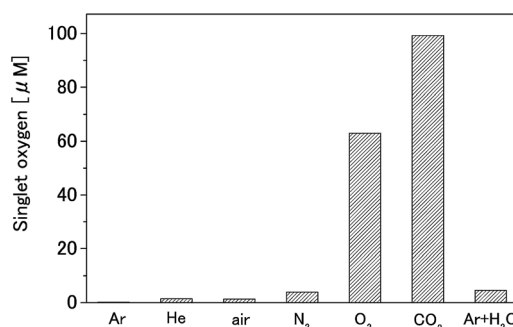

Fig. 1 Plasma treatment setup.

Fig. 2 Singlet oxygen production by each gas plasma (TPC is 75 mM, NaN$_3$ is 100 mM, plasma treatment time is 30 s).
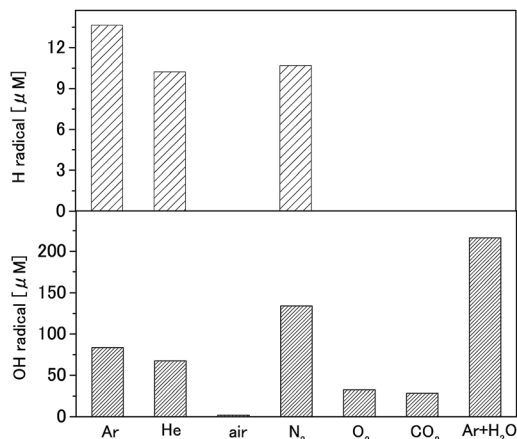
Fig. 3   OH and H radical production by each gas plasma (DMPO is 200 mM, plasma treatment time is 30 s).

productions were 14, 10, and 11 μM by argon, helium, and nitrogen plasmas, respectively.

Measurement of NO radicals

An MGD-Fe (8 mM) solution was treated with each gas plasma, and the amount of NO radicals generated was calculated from the ESR signal. Our results show that 1.6 μM of NO radicals was generated by air plasma. Although an NO radical spin adduct was obtained from the argon and helium plasmas, their ESR signal intensities were insufficient to calculate a production amount. NO radical production by the nitrogen, oxygen, and carbon dioxide plasmas were below the minimum detection limit.
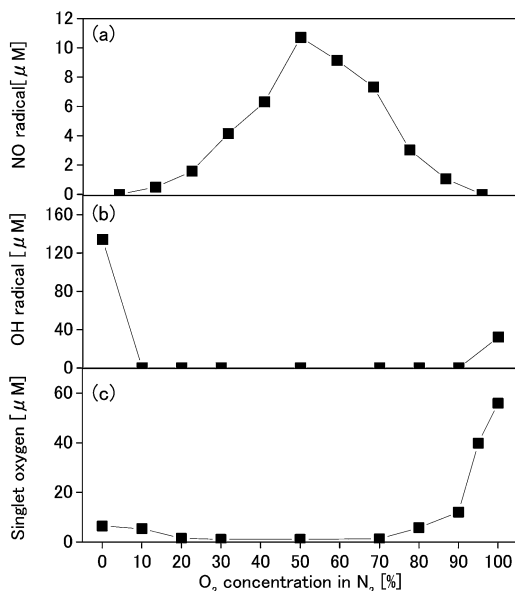

Fig. 4   Amount of singlet oxygen, OH radical, and NO radical production at differing concentrations of nitrogen–oxygen plasma ((a) MGD-Fe is 8 mM, (b) DMPO is 200 mM, (c) TPC is 75 mM, NaN$_3$ is 100 mM, plasma treatment time is 30 s).

Measurement of reactive species in nitrogen–oxygen mixture plasma

We investigated the generation of singlet oxygen, OH radicals, and NO radicals by the nitrogen–oxygen mixture plasma at specific volume ratios, and the results are shown in Fig. 4. NO radical production was highest for the mixed plasma with 50% oxygen in nitrogen, at 11 μM. This result was 6.9-fold higher than NO radical production by mock air plasma ($N_2 : O_2 = 8 : 2$). On the other hand, productions of singlet oxygen and OH radicals decreased, due to the mixed nitrogen and oxygen.

Discussion

In this study, concentration of each reactive species was determined by ESR signal; hence, the individual reactive species generated through a reaction process at the gas–liquid interface were caught by the spin-trapping reagent. We confirmed that each gas plasma emits an atomic line originating from its component species.[18] Therefore, the reactions relating to their respective reactive atomic species are expected to be those shown in Table 1. Except for mock air plasma, each gas plasma was observed to produce OH radicals. Argon, helium, and nitrogen, the inert gases, caused liquid phase reactions and OH radicals were generated by the reaction at the gas–liquid interface, as in Formulas (15)–(17). We assume that the large OH radical production by the nitrogen plasma was due to the lifetime of this reactive species. The atomic metastable lifetimes of various species are as follows: nitrogen $2^2D_{5/2}$: 6.1×10^4 s,[24]

Table 1   Production processes of reactive species under each condition

Reaction[a]	Rate constant (cm^3 s^{-1})	Reference
Electron impact reactions		
$Ar + e \rightarrow Ar^* + e$	$1.0 \times 10^{-11} T_e^{0.75} e^{-11.6/T_e}$	(1)[27]
$He + e \rightarrow He^*$	$f(T_e)$	(2)[28]
$O_2 + e \rightarrow {}^1O_2 + e$	$1.7 \times 10^{-9} e^{-3.1/T_e}$	(3)[29]
$O_2 + e \rightarrow 2O + e$	$7.1 \times 10^{-9} e^{-8.6/T_e}$	(4)[30]
$N_2 + e \rightarrow 2N + e$	$6.3 \times 10^{-6} e^{-9.8/T_e}$	(5)[31]
$CO_2 + e \rightarrow CO + O + e$		(6)[32]
$CO + e \rightarrow C + O + e$		(7)[33]
$H_2O + e \rightarrow H^\bullet + HO^\bullet + e$	$f(T_e)$	(8)[34]
Reactive species reactions		
$Ar^* + O_2 \rightarrow Ar + 2O$		(9)[35]
$He^* + O_2 \rightarrow He + 2O$		(10)[36]
$Ar^* + N_2 \rightarrow Ar + 2N$	1.6×10^{-11}	(11)[37]
$He^* + N_2 \rightarrow He + 2N$		(12)[38]
$N + O \rightarrow NO$		(13)[39]
$2O \rightarrow {}^1O_2$		(14)[29]
Liquid phase reactions		
$Ar^* + H_2O \rightarrow Ar + H^\bullet + HO^\bullet$		(15)[27]
$He^* + H_2O \rightarrow He + H^\bullet + HO^\bullet$		(16)[32]
$2N + 2H_2O \rightarrow N_2 + 2HO^\bullet$	2.5×10^{-10}	(17)[37]
$O + H_2O \rightarrow 2HO^\bullet$	$1.0 \times 10^{-11} T_e^{0.75} e^{-11.6/T_e}$	(18)[40]

[a] $f(T_e)$ indicates that the rate coefficient is obtained from EED using cross section from indicated reference.

argon 4^3P_2: 56 s,[25] oxygen 2^1D_2: 1.0×10^2 s,[24] and helium 2^3S_1: 7.9×10^3 s.[26] H radicals were also generated by argon, helium, and nitrogen plasma in the same amount of time as OH radicals according to formulas similar to (15)–(17).

Significant amounts of singlet oxygen were generated only by the oxygen and carbon dioxide plasmas. This suggests that oxygen and atomic oxygen, which is dissociated according to Formulas (4), (6), and (7), generate singlet oxygen as follows: (i) electron impact and oxygen recombines as in Formula (3) and (14), (ii) atomic oxygen and molecular oxygen combine and result in a dissociation reaction, and (iii) atomic oxygen and water molecules react. With this result, the amount of singlet oxygen produced by oxygen plasma is lower than that by carbon dioxide plasma. It seems that singlet oxygen generated in the atmosphere reacts with triplet oxygen to produce ozone; hence, oxygen plasma yields higher concentrations of triplet oxygen than carbon dioxide plasma. Mock air plasma containing oxygen gas generated neither singlet oxygen nor OH radicals. This is because the atomic oxygen and nitrogen generated in mock air plasma reacts to the NO radical through Formula (13).

We confirmed that OH radicals are generated by argon plasma; therefore, it is important to consider the reaction between argon plasma and water molecules in the gas phase. Thus, we made ESR measurements of argon with vapor plasma. Our results showed that the amount of OH radicals generated by argon with vapor plasma was higher than that by argon plasma alone. This suggests that Formula (8) directly accounts for part of the production by the plasma in addition to generating OH radicals, as in Formula (15). The reason for there being no detection of H radicals in this measurement is that generated argon ions react with H radicals to result in a protonated argon (ArH) in part of plasma production.

The process of NO radical production by each plasma can be explained as follows. When using nitrogen–oxygen mixture plasma, NO radicals are generated as in Formulas (4) and (5) through (17). With argon and helium plasmas, NO radicals are generated through a process involving oxygen and nitrogen in the atmosphere, as in Formulas (9) through (12). The reason the NO radical production by nitrogen, oxygen, and carbon dioxide plasmas were below the minimum detection limit was because producing atomic nitrogen or atomic oxygen from the atmosphere, as required for NO radical composition, is difficult by using these plasmas. These discussions are confirmed from the results shown in Fig. 4. When nitrogen and oxygen gases are mixed, the resulting mixed gas plasma can generate NO radicals; however, the productions of singlet oxygen and OH radicals are below minimum detection levels. The above results for the reactive species production by each plasma are summarized in Fig. 5.

Conclusions

Various gas plasmas were generated using a multi-gas plasma jet. The singlet oxygen, OH radicals, H radicals, and NO radicals, which were generated by each gas plasma, were investigated using ESR. We found that the largest amounts of singlet oxygen, OH radicals, H radicals, and NO radicals were generated by the carbon dioxide, argon with vapor, argon, and nitrogen–oxygen plasmas, respectively. Peak NO radical production occurred in the nitrogen gas plasma with 50% oxygen content.
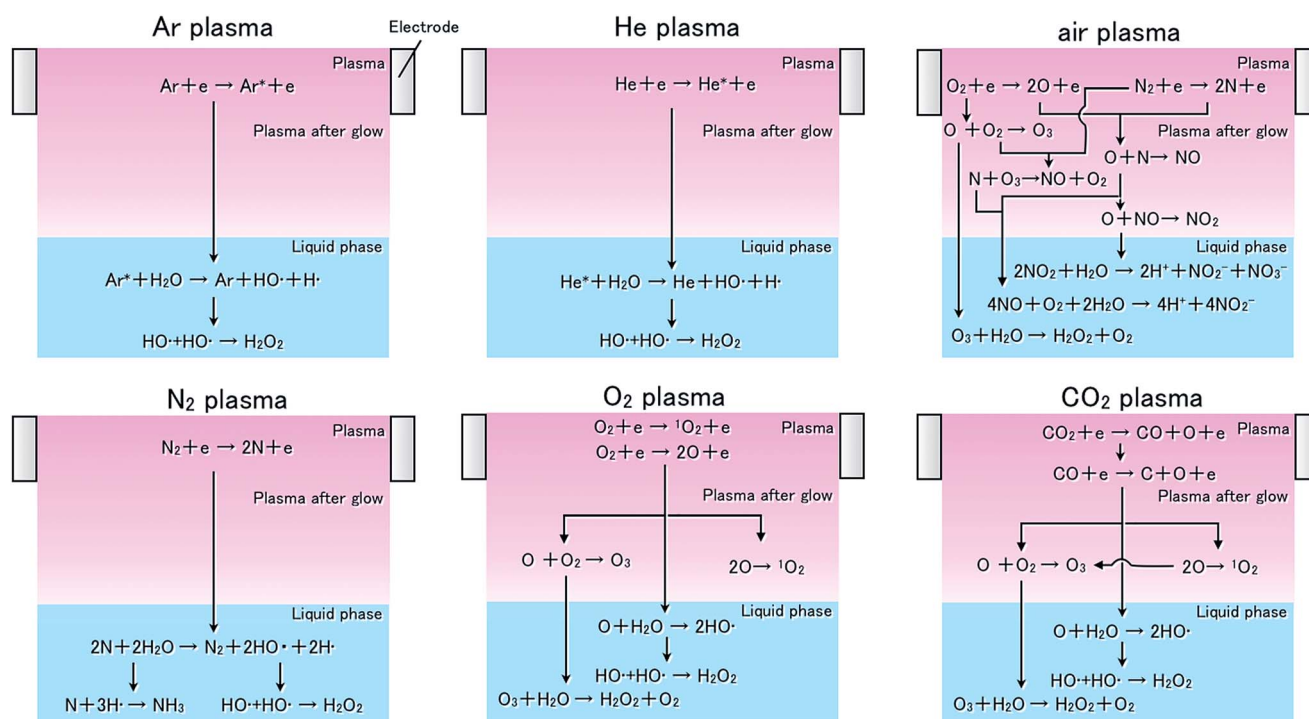

Fig. 5 Production processes of reactive species by each plasma treatment.

The amount of NO radicals produced at that ratio was 6.9-fold larger than those produced by mock air plasma. Given these facts, we found that the reactive species required for each application can be selectively generated by the plasma gas species chosen. Furthermore, the quantities required to generate the desired plasma effect can be estimated, and we could measure the amount of reactive species generated in this experiment. Our results suggest that the multi-gas plasma jet can provide partial explanations for plasma science mechanisms such as bacterial inactivation, cell growth, and blood coagulation.

Acknowledgements

Notes and references

1 W. Kumagai, H. Miyahara, E. Hotta and A. Okino, *Sixth Asian-European Int. Conf. Plasma Surf. Engineering*, 2007, vol. 310, p. 4007.

2 T. Tamura, Y. Kaburaki, R. Sasaki, H. Miyahara and A. Okino, *IEEE Trans. Plasma Sci.*, 2011, **39**, 1684.

3 T. Takamatsu, H. Miyahara, T. Azuma and A. Okino, *J. Toxicol. Sci.*, 2014, **39**, 281.

4 K. Shigeta, G. Köllensperger, E. Rampler, H. Traub, L. Rottmann, U. Panne, A. Okino and N. Jakubowski, *J. Anal. At. Spectrom.*, 2013, **28**, 637.

5 K. Shigeta, H. Traub, U. Panne, A. Okino, L. Rottmann and N. Jakubowski, *J. Anal. At. Spectrom.*, 2013, **28**, 646.

6 T. Iwai, Y. Takahashi, H. Miyahara and A. Okino, *Anal. Sci.*, 2013, **29**, 1141.

7 H. Miyahara, T. Iwai, Y. Nagata, Y. Takahashi, O. Fujita, Y. Toyoura and A. Okino, *J. Anal. At. Spectrom.*, 2014, **29**, 105.

8 J. Ehlbeck, U. Schnabel, M. Polak, J. Winter, T. von Woedtke, R. Brandenburg, T. von dem Hagen and K. D. Weltmann, *J. Phys. D: Appl. Phys.*, 2011, **44**, 013002.

9 S. U. Kalghatgi, G. Fridman, M. Cooper, G. Nagaraj, M. Peddinghaus, M. Balasubramanian, V. N. Vasilets, A. F. Gutsol, A. Fridman and G. Friedman, *IEEE Trans. Plasma Sci.*, 2007, **35**, 1559.

10 G. Fridman, M. Peddinghaus, H. Ayan, A. Fridman, M. Balasubramanian, A. Gutsol, A. Brooks and G. Friedman, *Plasma Chem. Plasma Process.*, 2006, **26**, 425.

11 S. Iseki, K. Nakamura, M. Hayashi, H. Tanaka, H. Kondo, H. Kajiyama, H. Kano, F. Kikkawa and M. Hori, *Appl. Phys. Lett.*, 2012, **100**, 113702.

12 M. Vandamme, E. Robert, S. Lerondel, V. Sarron, D. Ries, S. Dozias, J. Sobilo, D. Gosset, C. Kieda, B. Legrain, J. M. Pouvesle and A. L. Pape, *Int. J. Cancer*, 2012, **130**, 2185.

13 J. Heinlin, G. Morfill, M. Landthaler, W. Stolz, G. Isbary, J. L. Zimmermann, T. Shimizu and S. Karrer, *J. Dtsch. Dermatol. Ges.*, 2010, **8**, 968.

14 G. Lloyd, G. Friedman, S. Jafri, G. Schultz, A. Fridman and K. Harding, *Plasma Processes Polym.*, 2010, **7**, 194.

15 C. A. J. van Gils, S. Hofmann, B. K. H. L. Boekema, R. Brandenburg and P. J. Bruggeman, *J. Phys. D: Appl. Phys.*, 2013, **46**, 175203.

16 K. Oehmigen, J. Winter, M. Hahnel, C. Wilke, R. Brandenburg, K. D. Weltmann and T. Woedtke, *Plasma Processes Polym.*, 2011, **8**, 904.

17 Y. Sun, S. Yu, P. Sun, H. Wu, W. Zhu, W. Liu, J. Zhang, J. Fang and R. Li, *PLoS One*, 2012, **7**, e40629.

18 T. Takamatsu, H. Hirai, R. Sasaki, H. Miyahara and A. Okino, *IEEE Trans. Plasma Sci.*, 2013, **41**, 119.

19 T. Iwai, A. Albert, K. Okumura, H. Miyahara, A. Okino and C. Engelhard, *J. Anal. At. Spectrom.*, 2014, **29**, 464.

20 A. Tomaru, K. Hamasaki, R. Sasaki, H. Miyahara, A. Okino, N. Ogawa and K. Hamasaki, *PLoS One*, 2014, **9**, e85569.

21 Y. Matsumura, A. Iwasawa, T. Kobayashi, T. Kamachi, T. Ozawa and M. Kohno, *Chem. Lett.*, 2013, **42**, 1291.

22 M. Kohno, M. Yamada, K. Mitsuta, Y. Mizuta and T. Yoshikawa, *Bull. Chem. Soc. Jpn.*, 1991, **64**, 1447.

23 C. S. Lai and A. M. Komarov, *FEBS Lett.*, 1994, **345**, 120.

24 B. M. Smirnov, *Physics of Atoms and Ions*, ed. R. S. Berry, J. L. Birman, M. P. Silverman, H. E. Stanley and M. Voloshin, Springer, USA, 2003, p. 148.

25 N. E. Small-Warren and L.-Y. C. Chiu, *Phys. Rev. A*, 1975, **11**, 1777.

26 S. S. Hodgman, R. G. Dall, L. J. Byron, K. G. H. Baldwin, S. J. Buckman and A. G. Truscott, *Phys. Rev. Lett.*, 2009, **103**, 053002.

27 R. S. Mason, P. D. Miller and I. P. Mortimer, *Phys. Rev. E: Stat. Phys., Plasmas, Fluids, Relat. Interdiscip. Top.*, 1997, **55**, 7462.

28 E. Karakas, M. Koklu and M. Laroussi, *J. Phys. D: Appl. Phys.*, 2010, **43**, 155202.

29 A. A. Ionin, I. V. Kochetov, A. P. Napartovich and N. N. Yuryshev, *J. Phys. D: Appl. Phys.*, 2007, **40**, R25.

30 W. Bian, X. Song, D. Liu, J. Zhang and X. Chen, *Chem. Eng. J.*, 2013, **219**, 385.

31 V. Sharma, K. Hosoi, T. Mori and S. Kuroda, *Appl. Mech. Mater.*, 2013, **268–270**, 522.

32 M. Li, G. H. Xu, Y. L. Tian, L. Chen and H. F. Fu, *J. Phys. Chem. A*, 2004, **108**, 1687.

33 H. D. Hagstrum, *Rev. Mod. Phys.*, 1951, **23**, 185.

34 D. X. Liu, P. Bruggeman, F. Iza, M. Z. Rong and M. G. Kong, *Plasma Sources Sci. Technol.*, 2010, **19**, 025018.

35 K. Takechi and M. A. Lieberman, *J. Appl. Phys.*, 2001, **90**, 3205.

36 D. X. Liu, M. Z. Rong, X. H. Wang, F. Iza, M. G. Kong and P. Bruggeman, *Plasma Processes Polym.*, 2010, **7**, 846.

37 M. Moravej, X. Yang, M. Barankin, J. Penelon, S. E. Babayan and R. F. Hicks, *Plasma Sources Sci. Technol.*, 2006, **15**, 204.

38 J. M. Pouvesle, A. Bouchoule and J. Stevefelt, *J. Chem. Phys.*, 1982, **77**, 817.

39 J. T. Herron and D. S. Green, *Plasma Chem. Plasma Process.*, 2001, **21**, 459.

40 S. Kongmany, H. Matsuura, M. Furuta, S. Okuda, K. Imamura and Y. Maeda, *J. Phys.*, 2013, **441**, 012006.